

Strong enhancement of ultraviolet emission from ZnO films by V implantation

Chang Oh Kim, Dong Hee Shin, and Suk-Ho Choi^{a)}

Department of Applied Physics, College of Applied Science, Kyung Hee University, Yongin 446-701, Korea

K. Belay and R. G. Elliman

Department of Electronic Materials Engineering, Research School of Physical Sciences and Engineering, Australian National University, Canberra, Australian Capital Territory 0200, Australia

(Received 29 October 2010; accepted 17 February 2011; published 14 March 2011)

ZnO films were prepared on Si(100) wafers by rf sputtering and subsequently implanted with V ions to fluences of $(1, 2.5, 5, 10) \times 10^{15} \text{ cm}^{-2}$. The room-temperature ultraviolet photoluminescence (PL) intensity of the implanted films is shown to increase with increasing fluence up to $2.5 \times 10^{15} \text{ cm}^{-2}$, becoming ~ 37 times more intense than the emission from the unimplanted ZnO film, before decreasing at higher fluences. The increase in PL intensity is correlated with improved crystallinity of ZnO, accompanied by a reduction in the concentration of deep-level native defects by V incorporation into the ZnO lattice, as verified by x-ray diffraction, x-ray photoelectron spectroscopy, and low-temperature PL. The subsequent reduction in PL intensity at fluences higher than $2.5 \times 10^{15} \text{ cm}^{-2}$ is shown to result from the deterioration of the crystal quality and the precipitation of V secondary phase possibly introducing defects in the films. © 2011 American Vacuum Society. [DOI: 10.1116/1.3566529]

I. INTRODUCTION

ZnO is attractive for the fabrication of ultraviolet (UV) optoelectronic devices such as light-emitting diodes and laser diodes because of its direct-band structure, large band gap (3.479 eV), and high exciton binding energy (BE) (60 meV).^{1,2} This has led to a broad range of studies on the electrical, optical, and magnetic properties of ZnO thin films and specifically on transition-metal (TM)-ion-doped ZnO films.^{3–8} However, the material response to TM doping remains to be understood, with most reports concentrating on the ferromagnetic behavior of TM-doped films and the occasional study reporting on their luminescence properties.^{6,7}

ZnO films typically exhibit photoluminescence (PL) spectra in the visible and UV ranges. The UV PL is known to be due to near-band-edge (NBE) emission, while the visible PL is due to native defects in the material.^{9,10} Undoped ZnO films are *n*-type semiconductors having native defects such as oxygen vacancies (V_{O}), Zn vacancies (V_{Zn}), oxygen interstitials (O_i), Zn interstitials (Zn_i), and oxygen antisites (O_{Zn}), which significantly influence the visible PL.¹¹ However, their effect on the NBE PL is not well known. It has been reported that the excitonic emission from ZnO films is suppressed by doping with TM ions such as Cr, Co, V, Ti, Fe, Mn, and Ni, which is interpreted as being due to increased nonradiative recombination.⁶ In contrast, V-implanted ZnO films have shown intense white PL made up of different superimposed emission bands originating from intrinsic recombination of excitons and implantation-induced defects.⁷ In this article, we report strong enhancement of the band-edge UV PL from V-implanted ZnO films and show that this is correlated with

an increase in crystal quality of the ZnO, accompanied by a reduction in the concentration of deep-level (DL) native defects.

II. EXPERIMENT

The ZnO targets (99.999%) were mounted in a rf magnetron sputtering system and used to deposit ZnO films on *p*-type Si(100) substrates. Prior to use, the substrates were ultrasonically cleaned in acetone and alcohol, and then rinsed in de-ionized water. After the system was evacuated to a base pressure of 3×10^{-6} Torr, the substrates were presputtered at a power of 50 W for 10 min. The ZnO sputtering was then performed at room temperature (RT) for 50 min at a working pressure of 10^{-3} Torr. Other deposition conditions are as follows: rf power of 70 W, deposition rate of 2 nm/min, and gas mixing ratio of O_2/Ar of 1:8. The thickness of the films was estimated to be 100 nm by transmission electron microscopy. The ZnO films were subsequently implanted with 100 keV V^- ions to nominal fluences of $(1, 2.5, 5, 10) \times 10^{15} \text{ V cm}^{-2}$ at RT and subsequently annealed by rapid thermal annealing at temperatures (T_A) of 600–900 °C for 20 min in an O_2 atmosphere. The peak excess-V concentration for these implants was calculated from TRIM simulation to be in the range from 1.6×10^{20} to $1.6 \times 10^{21} \text{ V cm}^{-3}$ (0.2–1.9 at. %).¹²

PL spectra were measured using the 325 nm line of a He-Cd laser as the excitation source. The emitted light was collected by a lens and analyzed using a grating monochromator and a GaAs photomultiplier tube. Standard lock-in detection techniques were used to maximize the signal-to-noise ratio. The laser beam diameter was about 0.3 mm and the power density was about 2.12 W/cm^2 . X-ray photoelectron spectroscopy (XPS) measurements were performed at an en-

^{a)}Electronic mail: sukho@khu.ac.kr

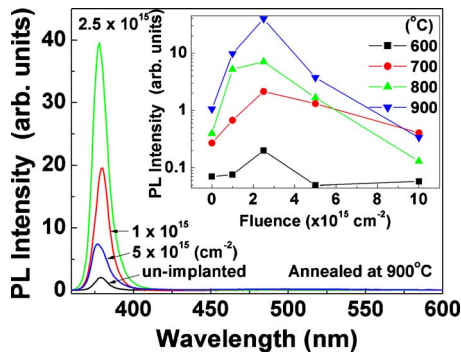


FIG. 1. (Color online) PL spectra at RT for unimplanted and V-implanted ZnO films after annealing at 900 °C. The intensities of all PL spectra except for a fluence of $2.5 \times 10^{15} \text{ cm}^{-2}$ were multiplied by 2 for better comparison. The inset summarizes the PL peak intensity as a function of fluence for various annealing temperatures.

ergy of 630 eV using the 8A1 beamline of Pohang Accelerator Laboratory. The total energy resolution of XPS was about 0.05 eV. Etching was performed *in situ* by sputtering the film with Ne^+ ions of energy 500 eV. The binding energy (BE) of the XPS spectra was calibrated by the peak of C 1s core level with a BE of 285 eV to correct for sample charging.

III. RESULTS AND DISCUSSIONS

Figure 1 shows PL spectra at RT for unimplanted and V-implanted ZnO films ($\text{ZnO}:\text{V}$) after annealing at 900 °C. For all samples the NBE-PL peaks are fixed at about 3.30 eV, independent of the implant fluence. The PL intensity of the $\text{ZnO}:\text{V}$ films increases with increasing fluence up to $2.5 \times 10^{15} \text{ cm}^{-2}$, becomes ~ 37 times larger than that of the unimplanted ZnO film at a fluence of $2.5 \times 10^{15} \text{ cm}^{-2}$, and then decreases with increasing fluence above $2.5 \times 10^{15} \text{ cm}^{-2}$. This fluence dependence is similar for all annealing temperatures, as shown in the inset of Fig. 1, although the PL intensity enhancement is greater at higher temperatures.

Figure 2(a) shows x-ray diffraction (XRD) spectra of $\text{ZnO}:\text{V}$ thin films as a function of fluence. The peak at a 2θ of $\sim 34.2^\circ$, which is attributed to the ZnO (002) reflection,¹³ is dominant for all samples. Significantly, the intensity of this peak also increases with increasing fluence up to $2.5 \times 10^{15} \text{ cm}^{-2}$ and decreases for fluences above this value, as summarized in Fig. 2(b). The full width at half-maximum (FWHM) of the XRD spectra shows a minimum value at $2.5 \times 10^{15} \text{ cm}^{-2}$, indicating that the crystal quality of the ZnO films can be improved by V implantation to fluences up to $2.5 \times 10^{15} \text{ cm}^{-2}$ and degraded by higher V fluences. There is also a slight shift in the 2θ value of the (002) reflection to lower values with increasing fluence (not shown here), possibly due to lattice distortions resulting from the incorporation of V ions in the ZnO lattice. For fluences significantly higher than $2.5 \times 10^{15} \text{ cm}^{-2}$ XRD analysis reveals an additional peak consistent with the formation of V secondary phase, $\text{Zn}_3(\text{VO}_4)_2$ (040) (JCPDS 34-0378), as previously reported.^{14,15} Thus, it can be inferred that the thermal solubility limit of V in ZnO for the samples in this work is less than or of order $8 \times 10^{20} \text{ V cm}^{-3}$.

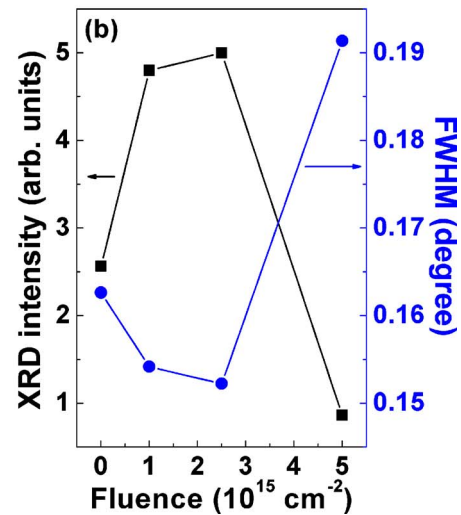
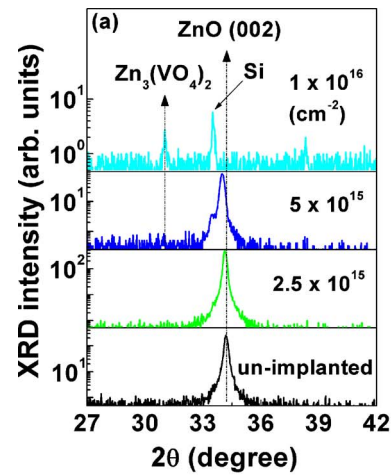


FIG. 2. (Color online) (a) XRD spectra of unimplanted and V-implanted ZnO films after annealing at 900 °C; (b) XRD intensity and FWHM as functions of fluence.

Figure 3(a) compares XPS spectra of $\text{ZnO}:\text{V}$ thin films with those of bare ZnO film. All spectra were obtained after removing 5 nm of the surface layer using Ne ion sputtering in order to avoid any possible influence of adsorbed contaminations. Following the same procedures presented before,¹⁰ the O 1s XPS peak could be fitted by two Gaussian-Lorentzian profiles centered at 530.7 and 532.2 eV, which are attributed to O^{2-} ions on the normal wurtzite structure of ZnO single crystal and O^{2-} in the oxygen-deficient regions within the matrix of ZnO, respectively.¹⁶ Therefore, the relative changes in the intensities of the two components may reflect the variations in the concentration of oxygen vacancies. The V 2p XPS spectra are split into a V 2p_{3/2} peak at 518 eV and a V 2p_{1/2} peak at 525 eV,^{17,18} both of which increase with increasing fluence. The XPS peak observed at around 10 eV for an unimplanted ZnO film is identified as the Zn 3d core level,^{19,20} as shown in the inset of Fig. 3(a).

Figure 3(b) summarizes the relative intensity of the fitted O 1s peaks (I_{531}/I_{532}) and the Zn 3d peak intensity as functions of fluence. The I_{531}/I_{532} value increases with increasing fluence up to $2.5 \times 10^{15} \text{ cm}^{-2}$ and decreases at higher flu-

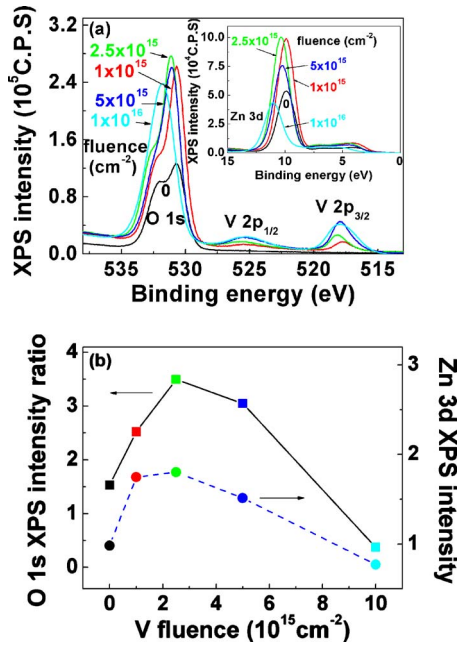


FIG. 3. (Color online) (a) O 1s and V 2p core-level XPS spectra of unimplanted and V-implanted ZnO films after annealing at 900 °C. The inset shows Zn 3d core-level XPS spectra. (b) Relative intensity of the fitted O 1s XPS peaks (I_{531}/I_{532}) and Zn 3d XPS intensity as functions of fluence.

ences. The Zn 3d peak similarly shows a maximum intensity at fluence = $2.5 \times 10^{15} \text{ cm}^{-2}$. These results suggest that the oxygen-deficient defects in ZnO matrix are minimized at a fluence of $2.5 \times 10^{15} \text{ cm}^{-2}$, thereby increasing the fraction of Zn–O bonds.

ZnO films have native defects such as vacancies, interstitials, and antisites (V_{O} , V_{Zn} , O_i , Zn_i , and O_{Zn}) that significantly influence their PL properties. Zn_i is known to form shallow-level defects, while others form DL defects.^{7,21} The DL defects could form nonradiative recombination channels, thereby reducing the NBE-PL intensity. As shown in Fig. 1, for V fluences less than $2.5 \times 10^{15} \text{ cm}^{-2}$, implantation with V, followed by annealing, appears to increase the NBE-PL intensity by reducing the concentration of nonradiative defects. As one possibility, the V_{O} density would decrease by occupation of oxygen atoms in the vacant sites during annealing under oxygen ambient, consistent with the enhancement of the O 1s XPS intensity ratio by the increase of V fluence up to $2.5 \times 10^{15} \text{ cm}^{-2}$, as shown in Fig. 3(b). During this process, the O_i density as well as the V_{O} density could decrease by the rearrangement of the atomic orientations. On the other hand, the decrease of the V_{O} density will result in the increase of stable Zn–O bonds,²⁰ consistent with the increased Zn 3d XPS intensity up to fluence = $2.5 \times 10^{15} \text{ cm}^{-2}$, as shown in Fig. 3(b). It has been reported that the incorporation of V would hinder zinc evaporation during the deposition of ZnO films, resulting in the decrease of V_{Zn} .¹⁷ All these processes would enhance the NBE-PL emission up to fluence = 2.5×10^{15} , as shown in Fig. 1.

The precipitation of the secondary phase could introduce defects into the ZnO films.^{22,23} These defects limit the radiative efficiency of the films and subsequently result in the

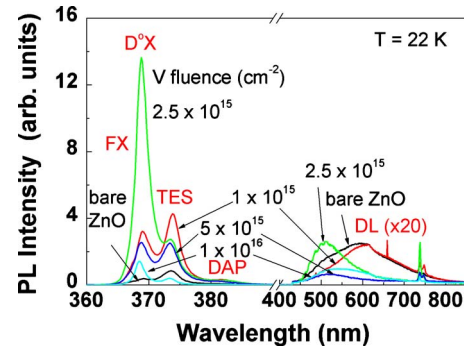


FIG. 4. (Color online) PL spectra at 22 K for unimplanted and V-implanted ZnO films after annealing at 900 °C.

decrease of the NBE emission at fluences $> 2.5 \times 10^{15} \text{ cm}^{-2}$, as shown in Fig. 1. The $\text{Zn}_3(\text{VO}_4)_2$ compound itself is known to produce a PL band at around 550 nm,¹⁵ which could be an evidence of its role for reducing the NBE PL.

PL was also measured at 22 K to see how the defect-related PL peaks vary with increasing V fluence, as shown in Fig. 4. Here, various PL peaks associated with free exciton (FX), neutral-donor-bound exciton (D^0X), two-electron satellite (TES) recombination of neutral-donor-bound exciton, donor-acceptor pair, and DL are indicated with reference to the previous publication.²⁴ As well known,^{24,25} the UV PL is dominated by the FX, D^0X , and TES recombinations at such low temperatures. These UV PL bands are combined into the NBE-PL emission at around RT.²⁶ Zn_i is known to form shallow-level defects,¹¹ and thus can be involved in the D^0X and TES recombinations. The DL PL is known to originate from other native defects.^{7,21} As can be shown from the PL spectra in Fig. 4, relative integrated PL intensity ratio (UV PL/DL PL) is largest at a fluence of $2.5 \times 10^{15} \text{ cm}^{-2}$. In other words, the DL defects are minimized at this fluence, consistent with the arguments proved by the XPS results, as explained above.

IV. CONCLUSION

ZnO films were grown on Si(100) wafers by rf sputtering, and subsequently implanted with V ions to fluences of 1×10^{15} – $10 \times 10^{15} \text{ V cm}^{-2}$. These ZnO:V films showed a maximum NBE-PL intensity at a fluence of around $2.5 \times 10^{15} \text{ cm}^{-2}$, which was ~ 37 times larger than that of the unimplanted ZnO film. These results were attributed to the improved crystallinity of ZnO and the reduction of deep-level native defects by V incorporation into the ZnO lattice. At fluence $> 2.5 \times 10^{15} \text{ cm}^{-2}$, the excess V precipitated as V-based secondary phases, thereby introducing defects into the ZnO films, and the crystal quality was degraded, resulting in the reduction of the NBE-PL intensity.

¹X. Ma, P. Chen, D. Li, Y. Zhang, and D. Yang, Appl. Phys. Lett. **91**, 021105 (2007).

²J.-H. Lim, C.-K. Kang, K.-K. Kim, D.-K. Hwang, and S.-J. Park, Adv. Mater. **18**, 2720 (2006).

³J. R. Neal, A. J. Behan, R. M. Ibrahim, H. J. Blythe, M. Ziese, A. M. Fox,

- and G. A. Gehring, *Phys. Rev. Lett.* **96**, 197208 (2006).
- ⁴Y. C. Yang, C. Song, F. Zeng, F. Pan, Y. N. Xie, and T. Liu, *Appl. Phys. Lett.* **90**, 242903 (2007).
- ⁵Q. Wang, Q. Sun, P. Jena, Z. Hu, R. Note, and Y. Kawazoe, *Appl. Phys. Lett.* **91**, 063116 (2007).
- ⁶S. Singh and M. S. Ramachandra Rao, *Phys. Rev. B* **80**, 045210 (2009).
- ⁷S. Müller, M. Lorenz, C. Czekalla, G. Benndorf, H. Hochmuth, M. Grudmann, H. Schmidt, and C. Ronning, *J. Appl. Phys.* **104**, 123504 (2008).
- ⁸S. Singh, N. Rama, K. Sethupathi, and M. S. Ramachandra Rao, *J. Appl. Phys.* **103**, 07D108 (2008).
- ⁹D. K. Lee, S. Kim, M. C. Kim, S. H. Eom, H. T. Oh, and S.-H. Choi, *J. Korean Phys. Soc.* **51**, 1378 (2007).
- ¹⁰S. Kim, D. K. Lee, S. H. Hong, S. H. Eom, H. T. Oh, S.-H. Choi, H. N. Hwang, and C. C. Hwang, *J. Appl. Phys.* **103**, 023514 (2008).
- ¹¹B. Lin, Z. Fu, and Y. Jia, *Appl. Phys. Lett.* **79**, 943 (2001).
- ¹²P. Biersack and L. G. Haggmark, *Nucl. Instrum. Methods Phys. Res. B* **174**, 257 (1980).
- ¹³Z. Z. Zhi, Y. C. Liu, B. S. Li, X. T. Zhang, Y. M. Lu, D. Z. Shen, and X. W. Fan, *J. Phys. D* **36**, 719 (2003).
- ¹⁴M. Kurzawa, I. Rychlowska-Himmel, M. Bosacka, and A. Blonska-Tabero, *J. Therm. Anal. Calorim.* **64**, 1113 (2001).
- ¹⁵S. Ni, X. Wang, G. Zhou, F. Yang, J. Wang, and D. He, *J. Alloys Compd.* **491**, 378 (2010).
- ¹⁶X. Q. Wei, B. Y. Man, M. Liu, C. S. Xue, H. Z. Zhuang, and C. Yang, *Physica B* **388**, 145 (2007).
- ¹⁷J. T. Luo, X. Y. Zhu, B. Fan, F. Zeng, and F. Pan, *J. Phys. D* **42**, 115109 (2009).
- ¹⁸L. Wang, L. Meng, V. Teixeira, S. Song, Z. Xu, and X. Xu, *Thin Solid Films* **517**, 3721 (2009).
- ¹⁹A. Bauknecht, U. Blieske, T. Kampschulte, J. Albert, H. Sehnert, M. Ch. Lux-Steiner, A. Klein, and W. Jaegermann, *Appl. Phys. Lett.* **74**, 1099 (1999).
- ²⁰R. A. Powell, W. E. Spicer, and J. C. McMenamin, *Phys. Rev. Lett.* **27**, 97 (1971).
- ²¹Ü. Özgür, Ya. I. Alivov, C. Liu, A. Teke, M. A. Reshchikov, S. Doğan, V. Avrutin, S.-J. Cho, and H. Morkoç, *J. Appl. Phys.* **98**, 041301 (2005).
- ²²M. Schumm, M. Koedel, S. Müller, C. Ronning, E. Dynowska, Z. Golaacki, W. Szuszkiewicz, and J. Geurts, *J. Appl. Phys.* **105**, 083525 (2009).
- ²³K. Potzger, S. Zhou, H. Reuther, K. Kuepper, G. Talut, M. Helm, J. Fassbender, and J. D. Denlinger, *Appl. Phys. Lett.* **91**, 062107 (2007).
- ²⁴B. K. Meyer, H. Alves, D. M. Hofmann, W. Kriegseis, D. Forster, F. Bertram, J. Christen, A. Hoffmann, M. Straßburg, M. Dworzak, U. Haboeck, and A. V. Rodina, *Phys. Status Solidi B* **241**, 231 (2004).
- ²⁵T. Voss, C. Bekeny, L. Wischmeier, H. Gafsi, S. Börner, W. Schade, A. C. Mofor, A. Bakin, and A. Waag, *Appl. Phys. Lett.* **89**, 182107 (2006).
- ²⁶Y.-H. Cho, J.-Y. Kim, H.-S. Kwack, B.-J. Kwon, L. S. Dang, H.-J. Ko, and T. Yao, *Appl. Phys. Lett.* **89**, 201903 (2006).